Supporting Information

Tronel et al. 10.1073/pnas.0914613107

SI Experimental Procedures

Lentivirus-Mediated Labeling of Neurons. The lentivirus-based lentiviral vector, pTRIPΔU3-MND-Dsred2-WPRE (Dsred2-LV), was produced by transient transfection of 293T cells according to standard protocols (1). In brief, subconfluent 293T cells were cotransfected with lentiviral genome (psPAX2) (2), with an envelope-coding plasmid (pMD2G-VSVG) and with vector constructs by calcium phosphate precipitation. Lentiviruses were harvested 40 h posttransfection and concentrated by ultracentrifugation. Titer (2.05×10^8 PFU·mL^{-1}) was determined on 293T cells as transducing units using serial dilutions of vector stocks.

Surgery. Rats were anesthetized with ketamine (60 mg/kg) and xylazine (7.5 mg/kg), and minipumps were implanted. In brief, a stainless steel cannula (28 gauge) connected by a catheter to the minipump was implanted into the left ventricle (bregma AP, −0.4 mm; lateral, 1.3 mm; vertical, 5 mm below the surface of the skull). Alzet 2002 osmotic pumps were filled with either aCSF or D-APV (30 mM) or MK 801 (2 mM) and then implanted in the scapula. Animals were injected with BrdU on the day after surgery and then allowed to recover for 7 days. The infusion was started on the day before the first training day. For virus infusions, the tooth bar was set at 5.5 mm above the interaural zero; coordinates were +3 mm posterior to bregma, ±2.6 mm lateral, and −4 mm below the surface of the dura. Then 3 μL of viral solution was injected at a rate of 0.375 μL/min.

Immunohistochemistry. Free-floating sections (50 μm) were processed in a standard immunohistochemical procedure to visualize BrdU (1:100; Dako), HH3 (1/2,000; Cell Signaling), fractin (1/5,000; BD PharMingen), eGFP (1/500; BD PharMingen), and synaptophysin (1/500, Boehringer). The number of IR cells in the DG was estimated using the optical fractionation method. BrdU-Dcx and GFP-IR neurons were visualized as described previously (3). Morphometric analysis of BrdU-Dcx and virus-labeled neurons was performed with a 100× objective using a semiautomatic neuron tracing system (Neurolucida; Microbrightfield). In brief, for each group, the neurons (at least 10 per brain) were selected based on the following criteria: neurons exhibited vertically orientated dendrites that extended into the dentate molecular layer, and dendrites of selected neurons had minimal overlap with the dendrites of adjacent cells, to allow unambiguous tracing of the dendritic tree. Data for various metric measurements, including cell body area, number of dendritic nodes, number of dendritic ends, and total dendritic length, were calculated. Then the spatial distribution of dendritic branches was analyzed using the concentric analysis of Sholl, performed using the Neuroexplorer component of the Neurolucida program. The data were reanalyzed by counting the number of occurrences of branch points in the dendritic arbor falling between concentric spheres separated by a fixed number of microns (25 μm).

The phenotype of BrdU-IR cells was examined by immunofluorescence double-labeling using rat anti-BrdU (1:500; Accurate Scientific) combined with a marker of mature neurons (NeuN, 1:1,000; Chemicon) revealed with, respectively, Cy3 goat anti-rat antibody (1:1,000; Jackson Laboratory) and Alexa-Fluor 488 goat anti-mouse (1:1,000; Invitrogen). At least 50 BrdU-IR cells per animal were analyzed using a confocal microscope (Leica DMR TCS SP2) with a plane apochromatic 63× oil lens (numerical aperture 1.4; Leica). All quantifications were performed by the same investigator, who was blinded to the experimental conditions.

For spine analysis, images of GFP-IR dendritic processes were acquired at 0.2-μm intervals with the SPE confocal system with a plane apochromatic 63× oil lens (numerical aperture 1.4; Leica) and a digital zoom of 2. Maximum projections of *z*-series were created with the Volocity software (Improvision). A 40-μm segment was traced on each dendrite, and the numbers of spines, lengths of spines, and sizes of the spine heads were determined. A total of 10 neurons from 5 rats from each group were analyzed (~1,000 spines).

1. Sena-Esteves M, Tebbets JC, Steffens S, Crombleholme T, Flake AW (2004) Optimized large-scale production of high titer lentivirus vector pseudotypes. *J Virol Methods* 122: 131–139.
2. Dull T, et al. (1998) A third-generation lentivirus vector with a conditional packaging system. *J Virol* 72:8463–8471.
3. Rao MS, Shetty AK (2004) Efficacy of doublecortin as a marker to analyse the absolute number and dendritic growth of newly generated neurons in the adult dentate gyrus. *Eur J Neurosci* 19:234–246.

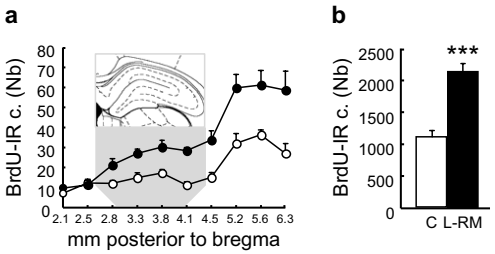

Fig. S1. (*A*) Septotemporal distribution of BrdU-IR cells. (*B*) Number of BrdU-IR cells in the septal region of the DG (t_{15}= −5.46; $P < 0.001$). C, control ($n = 6$), L-RM, learning RM ($n = 11$). ***$P \leq 0.001$ compared with control.

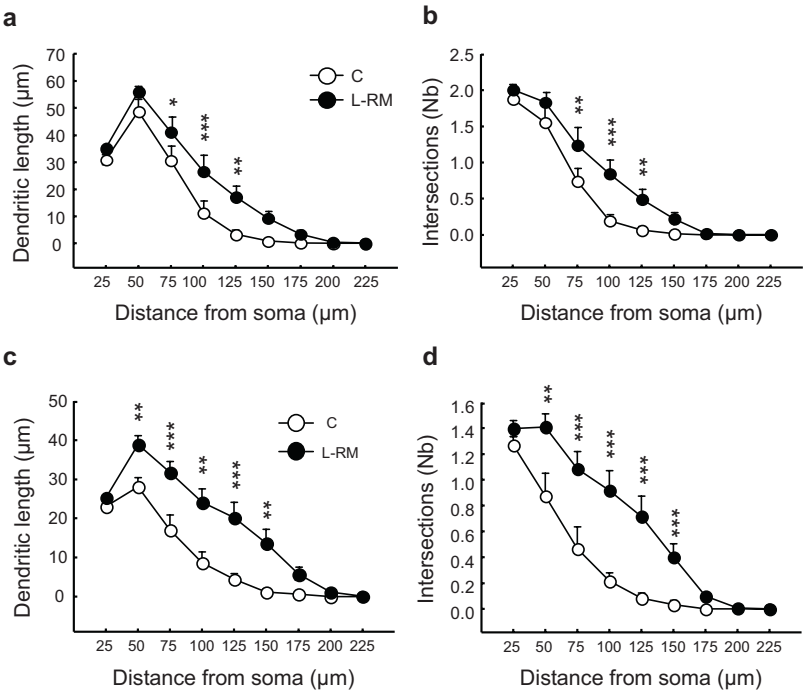

Fig. S2. Spatial learning increases the complexity of the dendritic arbor of adult-born neurons selected by learning. (*A* and *B*) Sholl analysis of the dendritic length ($F_{8,120} = 5.14$; $P < 0.001$) (*A*) and of the number of intersections ($F_{7,105} = 4.86$; $P < 0.001$) (*B*) of new neurons born 1 week before learning. (*C* and *D*) Sholl analysis of the dendritic length ($F_{8,88} = 2.30$; $P < 0.05$) (*C*) and the number of intersections ($F_{8,88} = 2.66$; $P < 0.05$) (*D*). *$P \leq 0.05$; **$P \leq 0.01$; ***$P \leq 0.001$ compared with controls.

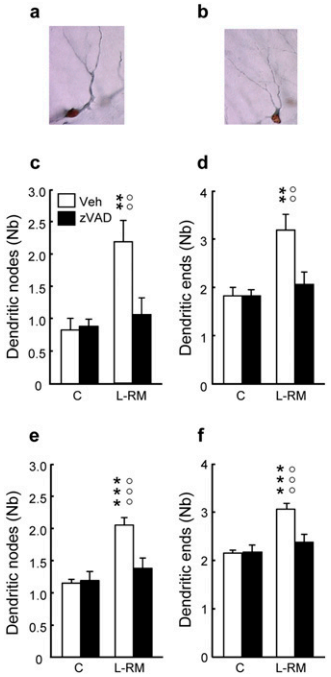

Fig. S3. Homeostatic regulation of the dendritic arbor of adult-born neurons by spatial learning. Examples of IdU-Dcx-IR cell (*A*) and CldU-Dcx-IR cell (*B*) of a Z-VAD-treated animal. (*C* and *D*) Effects of zVAD and vehicle treatments on the number of nodes ($F_{3,25} = 6.36$; $P = 0.002$) (*C*) and the number of ends of IdU-Dcx-IR dendrites ($F_{3,25} = 6.47$; $P = 0.002$) (*D*). (*E* and *F*) Effects of zVAD and vehicle treatments on the number of nodes ($F_{3,25} = 11.91$; $P < 0.001$) (*E*) and the number of ends of CldU-Dcx-IR dendrite cells ($F_{3,25} = 11.95$; $P < 0.001$) (*F*). C, control (Veh, $n = 6$; zVAD, $n = 6$); L-RM, learning RM (Veh, $n = 10$; zVAD, $n = 7$); Vehicle, □; zVAD, ■. **$P \leq 0.01$; ***$P \leq 0.001$ compared with control Veh. °°$P \leq 0.01$; °°°$P \leq 0.001$ compared with zVAD group.

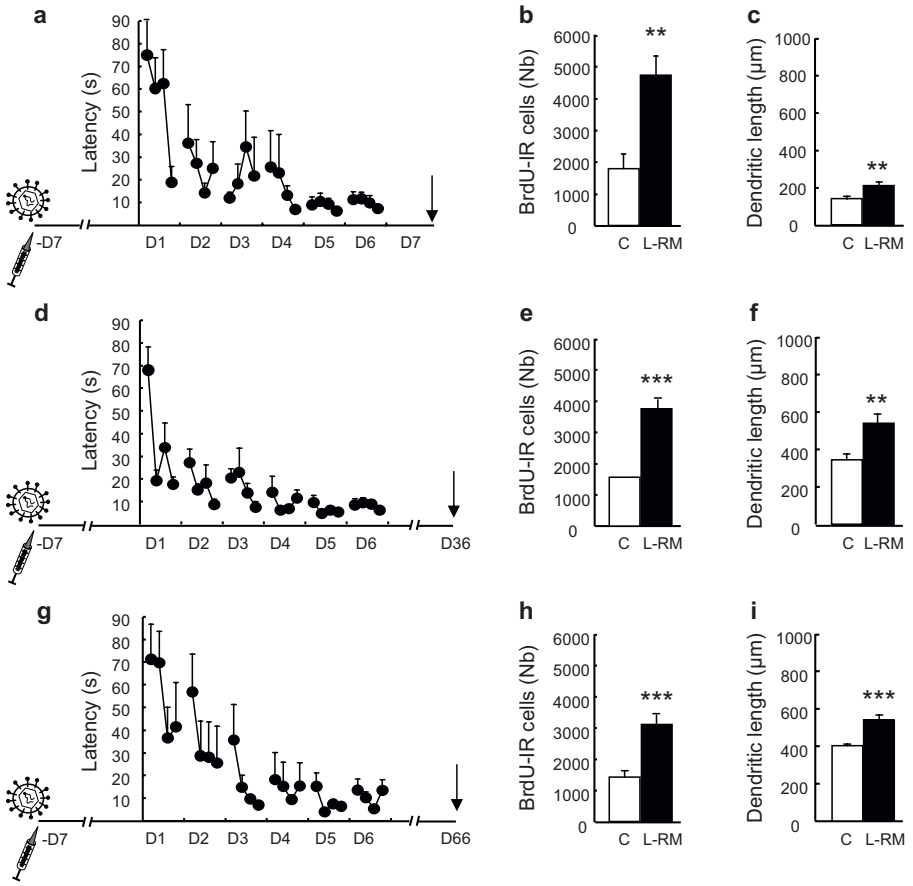

Fig. S4. The effect of spatial learning on the dendritic arbor is long lasting. (*A*, *D*, and *G*) Latency to find the escape platform. The symbol represents retrovirus infusions; the syringe, BrdU injection; the arrows, times of sacrifice. (*B*, *E*, and *H*) Total number of BrdU-IR cells. (*C*, *F*, and *I*) Length of dendrites. C, control (1D, $n = 9$; 1M, $n = 8$; 2M, $n = 7$); L-RM, learning RM (1D, $n = 8$; 1M, $n = 8$; 2M, $n = 9$).**$P \leq 0.01$; ***$P \leq 0.001$ compared with control.

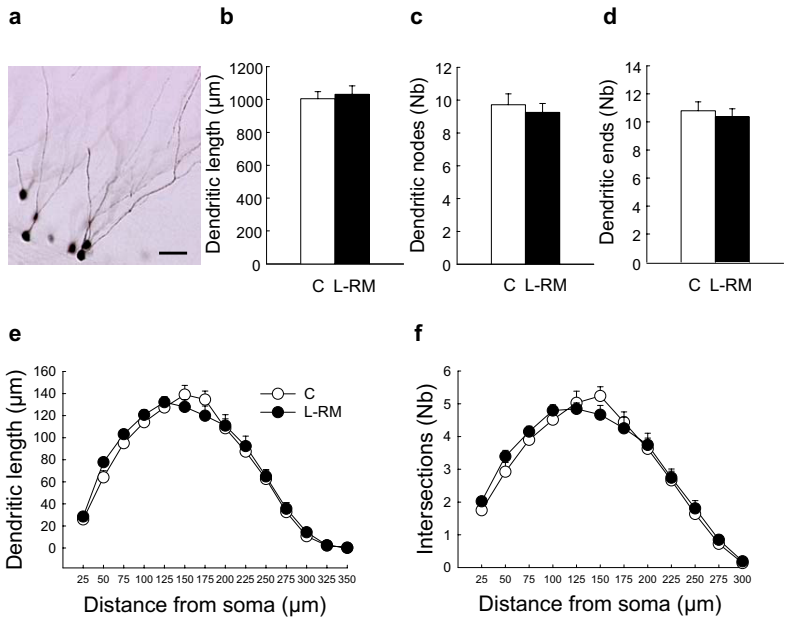

Fig. S5. Spatial learning has no effect on the dendritic arbor complexity of mature neurons. (*A*) Mature neurons labeled with the Dsred2 lentivirus. (*B*) Length of the dendritic arbor. (*C*) Number of nodes. (*D*) Number of endings. (*E* and *F*) Sholl analysis of the dendritic length (*E*) and the number of intersections (*F*). C, control ($n = 8$); L-RM, learning RM ($n = 14$). (Scale bar: 25 μm.)

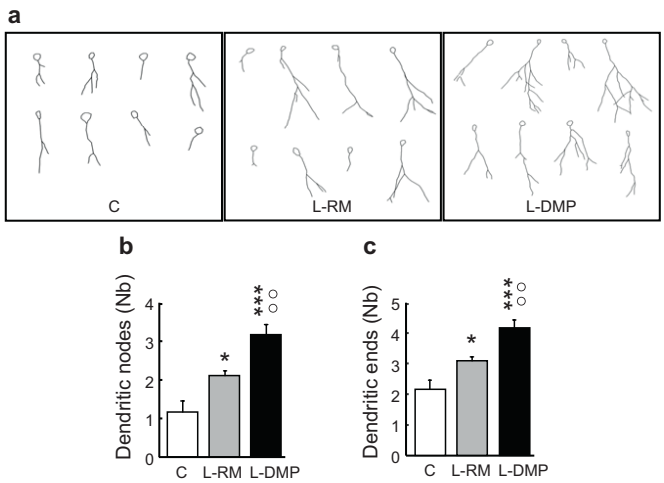

Fig. S6. Effect of the cognitive demand on the dendritic arbor complexity of adult-born neurons. (*A*) Examples of neuron tracings for one animal of each group. (*B*) Number of nodes ($F_{2,21}$ = 14.017; $P < 0.001$). (*C*) Number of endings ($F_{2,21}$ = 14.22; $P < 0.001$). C, control (n = 8); L-RM, learning RM (n = 8); L-DMP, learning DMP (n = 8). *$P \leq 0.05$; ***$P \leq 0.001$ compared with control. °°$P \leq 0.01$ compared with L-RM.

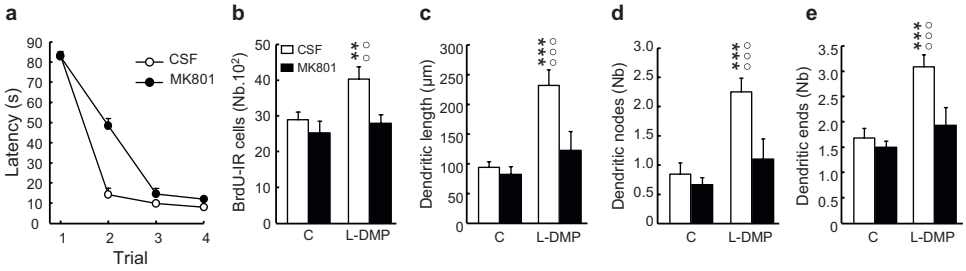

Fig. S7. Influence of NMDA receptors antagonist MK-801 on spatial learning and learning-induced changes in dendritic arbor complexity. (*A*) Latency to find the escape platform ($F_{3,16}$ = 5.44; $P < 0.01$). (*B*) Total number of BrdU-IR cells ($F_{3,16}$ = 5.44, $P < 0.01$). (*C*) Length of the dendritic arbor ($F_{3,16}$ = 13.35, $P < 0.001$). (*D*) Number of nodes ($F_{3,16}$ = 12.57, $P < 0.001$). (*E*) Number of endings ($F_{3,16}$ = 12.57, $P < 0.001$). C, control (CSF, n = 5; MK801, n = 5); L-DMP, learning DMP (CSF, n = 5; MK801, n = 5). Vehicle, □; MK801, ■. **$P \leq 0.01$; ***$P \leq 0.001$ compared with control. °°$P \leq 0.01$; °°°$P \leq 0.001$ compared with the MK801 group.

Table S1. Summary of the procedures

	Experiment	Days of XdU or retrovirus injections in respect to training days (Dn)	Group size	Duration of training	Time of sacrifice in respect to the start of training
1a	Influence of RM learning on neoneurons born 1 week before exposure to the task	BrdU on –D7	C = 6; L-RM = 11	6 days	Seventh day
1b	Influence of RM learning on neoneurons born during the early phase of training	BrdU on D1–D4	C = 6; L-RM = 7	8 days	Ninth day
2	Effect of zVAD infusion on learning-induced dendritic changes	IdU on –D7; CldU on –D3	C Veh = 6; L-RM Veh = 10 Cz VAD = 6; L-RMz VAD = 7	6 days	Seventh day
3	Time-course study of learning-induced dendritic changes	GFP-retrovirus infusion on –D7	C = 9; L-RM = 8	6 days	Seventh day
	Time-course study of learning-induced dendritic changes	GFP-retrovirus infusion on –D7	C = 8; L-RM = 8	6 days	36th day
	Time-course study of learning-induced dendritic changes	GFP-retrovirus infusion on –D7	C = 7; L-RM = 9	6 days	66th day
	Time-course study of learning-induced dendritic changes	GFP-retrovirus infusion on –D7	C = 7; L-RM = 8	6 days	96th day
4	Influence of learning on mature neurons	Dsrd-lentivirus infusion on –D7	C = 8; L-RM = 14	6 days	Seventh day
5	Influence of the cognitive demand	BrdU on –D7	C= 8; L-RM = 8; L-DMP = 8	6 days	Seventh day
6	Role of NMDA receptors (APV)	BrdU on –D7	C CSF= 7; L-DMP CSF= 10; C APV = 9; L-DMP APV = 9	9 days	10th day
	Role of NMDA receptors (MK801)	BrdU on –D7	C CSF= 9; L-DMP CSF= 7; C MK801 = 5; L-DMP MK801 = 5	9 days	10th day

Table S2. Morphological analysis of GFP-IR neurons of animals of the L-RM and control groups

	Group		
Delay between training and sacrifice	Control	L-RM	Statistical significance
Cell body (area)			
1D	44.84 ± 1.60	47.35 ± 2.85	$t_{15} = -0.7$; $P = 0.4$
1M	57.74 ± 2.38	60.16 ± 1.94	$t_{14} = -0.8$; $P = 0.44$
2M	58.50 ± 3.25	66.43 ± 2.04	$t_{14} = -2.16$; $P = 0.05$
3M	71.38 ± 1.96	70.67 ± 3.62	$t_{14} = 0.16$; $P = 0.87$
Nodes (Nb)			
1D	1.17 ± 0.14	2.27 ± 0.16	$t_{15} = -4.17$; $P < 0.001$
1M	2.48 ± 0.24	5.22 ± 0.61	$t_{14} = -7.49$; $P < 0.001$
2M	3.32 ± 0.15	6.19 ± 0.31	$t_{14} = -7.7$; $P < 0.001$
3M	3.74 ± 0.36	6.39 ± 0.50	$t_{14} = -4.16$; $P < 0.001$
Ends (Nb)			
1D	2.15 ± 0.15	3.28 ± 0.16	$t_{15} = 5.22$; $P < 0.001$
1M	3.58 ± 0.26	6.25 ± 0.59	$t_{14} = -4.30$; $P < 0.001$
2M	3.51 ± 0.25	7.22 ± 0.33	$t_{14} = -7.74$; $P < 0.001$
3M	4.33 ± 0.16	7.56 ± 0.49	$t_{14} = -7.21$; $P < 0.001$
Length (μm)			
1D	140.22 ± 13.67	214.48 ± 17.67	$t_{15} = -3.36$; $P < 0.01$
1M	337.32 ± 30.28	538.72 ± 49.39	$t_{14} = -3.47$; $P < 0.01$
2M	396.10 ± 13.56	657.72 ± 23.51	$t_{14} = -8.90$; $P < 0.001$
3M	443.04 ± 21.7	738.61 ± 63.42	$t_{13} = -4.16$; $P < 0.001$